Nano Energy 90 (2021) 106501

Contents lists available at ScienceDirect

Nano Energy

journal homepage: www.elsevier.com/locate/nanoen

Self-sustainable flow-velocity detection via electromagnetic/triboelectric hybrid generator aiming at IoT-based environment monitoring

Quan Zhang[a,c,1], Long Li[a,b,c,d,1], Tianhong Wang[a,b,c,1], Yichen Jiang[a,b,c], Yingzhong Tian[a,b], Tao Jin[a,b,c,*], Tao Yue[a,c,d,*], Chengkuo Lee[e,f,g,**]

[a] School of Mechatronic Engineering and Automation, Shanghai University, Shanghai 200444, China
[b] Shanghai Key Laboratory of Intelligent Manufacturing and Robotics, Shanghai University, Shanghai 200444, China
[c] School of Artificial Intelligence, Shanghai University, Shanghai 200444, China
[d] Shanghai Institute of Intelligent Science and Technology, Tongji University, Shanghai 200092, China
[e] Department of Electrical and Computer Engineering, National University of Singapore, 4 Engineering Drive 3, Singapore 117576, Singapore
[f] Center for Intelligent Sensors and MEMS (CISM), National University of Singapore, 5 Engineering Drive 1, Singapore 117608, Singapore
[g] National University of Singapore Suzhou Research Institute (NUSRI), Suzhou Industrial Park, Suzhou 215123, China

ARTICLE INFO

Keywords:
Triboelectric nanogenerator
Electromagnetic generator
Self-powered sensor
Environment monitoring
Internet of things (IoT)

ABSTRACT

Harvesting energy from the environment has aroused widespread interest and it can supply renewable power to achieve sustainable environment monitoring for the Internet of things (IoT). In this paper, a tri-cylinder-like hybrid generator composed of triboelectric nanogenerator (TENG) and electromagnetic generator (EMG) is presented to harvest the mechanical energy produced by various fluids as well as sense the real-time flow velocity ecofriendly. This generator can be driven to rotate through a windmill or waterwheel, leading to the reciprocating sliding of the internal spring-magnet structure. By arranging coil and foldable TENG structure, it can generate hybrid signals along with the rotation while gear pairs are further utilized for both boosting the output and expanding the sensing range. The experimental result shows more than twice and six times output can be realized by gear pairs for TENG and EMG, respectively, and the recognizable rotational frequency reaches 10 Hz with a transmission ratio of 5:1. The rotation speed and direction detection are realized based on the output voltage frequency and value of TENG caused by the difference of triboelectric layer number. Combined with two hybrid generators in a vertical layout, the wind directions are also investigated to be distinguished by computing the signal characteristics. Based on these sensing mechanisms, this hybrid generator is able to achieve wireless sensing as EMG boosted by gear pairs is sufficient to supply the energy for wireless transmission. This self-sustained sensory system shows its great potential for unmanned environment monitoring, disaster warning as well as the meteorological record in IoT applications.

1. Introduction

Environment monitoring including the record of wind scale, rainfall and water level by an unmanned weather station plays an important role in the future since there requires the meteorological information for daily weather prediction and early warning to avoid the disasters [1–3]. For example, the heavy rainfall in a short period often leads to a surge in river flow, which in turn often foreshadows sudden regional natural disasters. Meanwhile, with the rapid development of 5G and the Internet of things (IoT), the sensory information can be transmitted with an ignorable delay and thus smart meteorological prediction can be realized through remote terminals with big data and cloud computing techniques [4–10]. However, the feasibility and cost-effectiveness of unmanned weather stations have to be considered as the battery replacement and complex wire distribution are required to ensure the daily operation in an outdoor environment [11–13]. Furthermore, the necessary maintenance for remote locations like grassland and mountainous region will arise unexpected difficulties. Thus, besides the

* Corresponding authors at: School of Mechatronic Engineering and Automation, Shanghai University, Shanghai 200444, China.
** Corresponding author at: Department of Electrical and Computer Engineering, National University of Singapore, 4 Engineering Drive 3, Singapore 117576, Singapore.
E-mail addresses: jt233@shu.edu.cn (T. Jin), tao_yue@shu.edu.cn (T. Yue), elelc@nus.edu.sg (C. Lee).
[1] These authors contributed equally to this work.

https://doi.org/10.1016/j.nanoen.2021.106501
Received 26 June 2021; Received in revised form 19 August 2021; Accepted 6 September 2021
Available online 20 September 2021

real-time information collection and monitoring, the next-generation unmanned weather station should be energy-sustainable and can realize the wireless transmission for avoiding additional batteries and electrical wires. The self-powered device capable of harvesting energy from ambience to support its basic operation emerges as a possible solution [14–17].

Recently, triboelectric nanogenerators (TENGs), a novel technology based on the coupling of triboelectrification and electrostatic induction, have been successfully developed and attracted increasing interest [18–21]. Due to its unique operation principle, TENG always exhibits the significant merits of light-weight structure, fabrication simplicity, high power density, outstanding energy conversion ratio, and low material limitation. In addition, based on its ultrahigh sensitivity to mechanical stimulus, the output electrical signal generated during energy collection can be utilized directly for further information interaction [22–25]. Thus, a variety of TENG-based devices with different working modes have been investigated as self-powered sensors for IoT applications such as wearable electronics [26–31], human-machine interface [32–35] and robotic sensing [36–39]. As for the scenarios for the unmanned weather station, fluid flows including wind and waterflow are regarded as a potential and sustainable energy source [40–42] and thus it becomes an intriguing approach to obtain the flow velocity for both wind and waterflow based on self-powered TENG sensors to predict the weather condition as well as the flood situation. Although some previous works have achieved self-powered fluid speed detection [43–45], there still have some difficulties in broadband detection by single TENG sensor. For instance, the TENG-based device may exhibit low output for the extremely low frequency like 0.2 Hz and the inertia of the structure will limit the device to work under higher frequency for wind detection [46]. In this case, a single structure often can't meet the requirements of various application scenarios [47], and there require some techniques to adjust the working frequency to obtain a stable and higher output.

Wireless transmission is another vital point to construct the unmanned weather station in order to reduce the extra accessory requirement [48–50]. Although TENG-based sensors can work without any power consumption and several kinds of measures have been proposed to strengthen the output performance, e.g., surface treatment and charge injection [51–54], it is not sufficient to satisfy the required power of wireless circuit by only using a comparable compact structure. Thus, except for expanding the contact area by structural design or long-time energy charging, there still requires a breakthrough for improving the energy harvesting efficiency of the self-powered system. Note that except for triboelectricity, various methods have been used to transform fluid energy into electricity based on different mechanisms such as electromagnetic [55–57], electrostatic [58–60] and piezoelectric effect [61–63]. Among them, electromagnetic generators (EMGs) can provide higher current than TENG. Hence, an optimized solution is to design the hybrid generator with a combination of TENG and EMG, where TENG for sensing and both generators for energy harvesting in order to support the self-sustained wireless data transmission, showing its potential for unmanned weather station [64–67].

In this work, we report a tri-cylinder-like TENG-EMG hybrid generator to act as a self-powered rotational sensor for fluid velocity detection as well as an energy harvester for wireless transmission. The spring-magnet structure is arranged in a cylinder where the coil of EMG and foldable TENG are arranged to realize energy conversion during magnet movement. Three cylinders in a circle form the rotational sensor and the triboelectric layer number in each cylinder is different. Thus, the real-time velocity can be calculated by the intervals between the triboelectric signals while the sequence of voltage represents the rotational direction. Besides, gear pairs with different transmission ratios are introduced to strengthen the output and expand the sensing range. Owing to this mechanism, the hybrid generator shows more than twice and six times output for TENG and EMG respectively under 1 Hz, and the recognizable rotational frequency reaches 10 Hz with a transmission ratio of 5:1. Then, self-powered devices for wind and waterflow speed detection are demonstrated for weather monitoring, and two hybrid generators with vertical layout are developed to distinguish the wind direction by computing the signal ratio. The hybrid generator is also able to achieve wireless sensing as EMG boosted by gear pairs is sufficient to supply the energy. This self-sustained sensory system shows its great potential for unmanned environment monitoring, disaster warning as well as the meteorological record in IoT applications.

2. Results and discussion

The hybrid generator consisting of three TENG-EMG modules for rotational sensing is illustrated in Fig. 1a. Due to the great influence of environmental humidity on the output, TENG needs to be packaged by the enclosed structure and thus, a single module is fabricated using an acrylic tube to envelop the spring and magnet slider (weight = 300 g). For generating the triboelectric signal and the induced current along with the magnet's sliding, a sandwiched TENG structure is arranged on the distal end of the tube where Cu wire is tightly wrapped (Fig. 1b–c). Here, the silicone rubber (Ecoflex 00-50) is selected as the negatively triboelectric material with a layer of conductive nickel cloth (Ni-cloth) on its back as the electrode. The silicone rubber is pretreated with sandpaper to construct the microstructure to increase the output. The PET with the thickness of 1 mm acts as the substrate as well as the skeleton to offer the self-recovery force for TENG, and the negative triboelectric patch is glued to the PET substrate directly. Meanwhile, another layer of Ni-cloth is used as the positive friction material, which is arranged opposite to the silicone rubber. All the TENG-EMG modules are distributed onto the central component at the angle of 120° and the number of triboelectric layers is different in each module. Thus, as the hybrid generator rotates, the magnet will slide along with the tube and be pulled back by the spring successively. Accordingly, the rotational speed and direction can be distinguished by calculating the time interval between two peaks and analyzing distinct voltage sequences, respectively.

For mechanical energy in the different forms of fluids, there exist differences in the frequency range. The waterflow in nature always exhibits a narrower speed range, and a relatively stable velocity, whereas the measurement of wind speed requires higher frequency and accuracy. As shown in Fig. 1d–e, the designed hybrid generator combined with waterwheel and windmill can be used for fluid speed detection, where the windmill has a gear pair with 5:1 transmission ratio. As the installation of the gear pair, the hybrid generator-based sensor will be slowed down under the same wind condition and the rational angle of the windmill should be multiplied by the transmission ratio. Despite that the sensing range of the sensor is limited by the spring-mass structure due to the combination of gravity and centrifugation, the working frequency is expanded as the application of gear pair. In addition, the slow waterflow can be accelerated by the gear pair with a reverse transmission ratio for increasing the output since both the TENG and EMG can be strengthened as the magnet operates at a higher speed. Thus, besides energy harvesting, the hybrid generator together with the gear pair can realize the unmanned environment monitoring since rainfall is related to the waterflow in nature and the wind scale can match with the signal frequency. Furthermore, the real-time meteorological information can be transmitted back to the remote terminal node for message feedback and decision-making through wireless by leveraging the IoT technology (Fig. 1f). As shown in Fig. 1g, the schematic diagram of the hybrid generator network is depicted for harvesting fluid energy to power the environmental monitoring. This self-sustained sensory system shows its great potential for the applications of unmanned environment monitoring, disaster warning as well as meteorological record.

The working mechanisms of the TENG-EMG hybrid generator are given in Fig. 2a–c. The device operation can be divided into four states marked as the states (i)–(iv) related to the working process of TENG as shown in Fig. 2b. The magnet is under centrifugal force along the sliding direction, pulling force in the opposite direction, and gravity in every

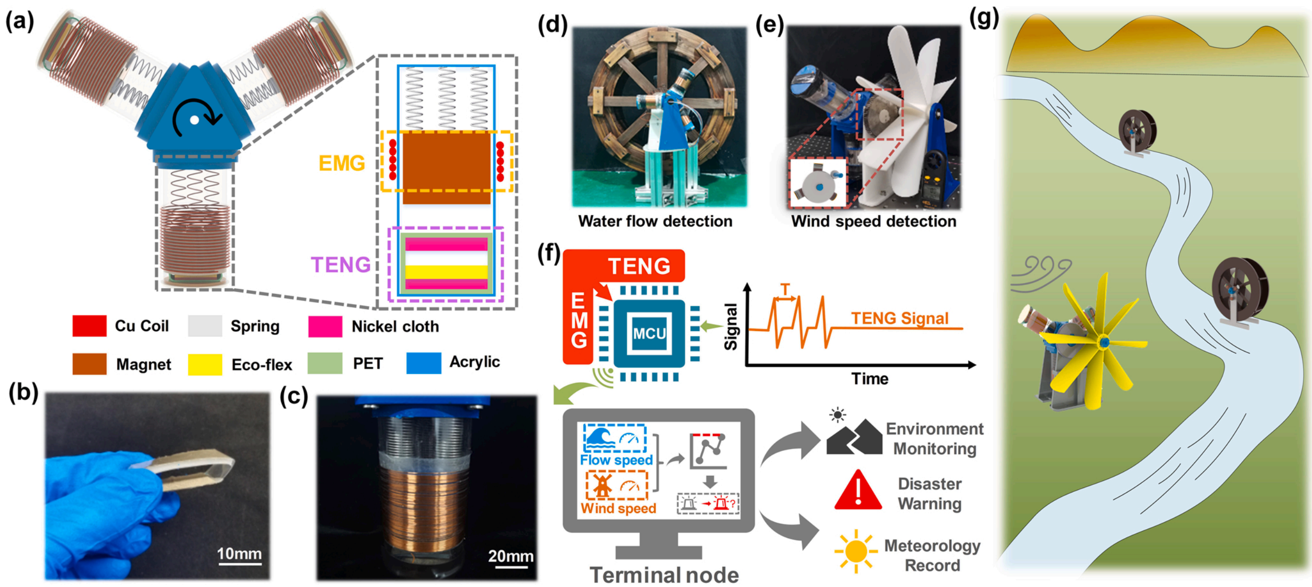

Fig. 1. The tri-cylinder-shaped triboelectric sensory system for unmanned environment monitoring. (a) Schematic illustration of the TENG-EMG hybrid generator. (b) Photograph of the TENG structure. (c) The as-fabricated cylinder with TENG and EMG. (d) The hybrid generator attached to a waterwheel for detecting the waterflow velocity, and (e) attached to a windmill for wind speed detection. (f) Diagram of the self-powered wireless sensory system based on TENG-EMG hybrid generator for environment monitoring and natural disaster warning. (g) Schematic diagram of the hybrid generator group for harvesting energy and environment monitoring.

state (Fig. 2a). In general, for the EMG-TENG module, the TENG should be compressed in the bottom position to ensure the charge transfer (i.e., the centrifugal force together with spring force is smaller than the gravity) while it needs to be released at the top position (i.e., the centrifugal force is smaller than the summary of gravity and spring force). Thus, the spring stiffness and magnet mass determine the working capability, and the detailed discussion for selection of mass and spring can be found in Supplementary materials Note 1. Here, the NdFeB magnet with a weight of 300 g and three springs with a spring coefficient of 30 N/m are selected to guarantee the operation under 2.5 Hz. In addition, the spring with various elastic coefficients can be chosen for adjusting the measurable range, e.g., improving spring stiffness for operation in a higher frequency.

The single TENG-EMG module moves in a circle and the TENG works in the contact-separation mode. The working process of TENG can be divided into states (i)–(iv) as shown in Fig. 2b. As the magnet compresses the TENG, it arrives to state (i) and two triboelectric layers contact with each other. Because of the electron's affinity difference, the surface of silicone rubber will be negatively charged and the top layer of Ni-cloth will be positively charged. When the compression is releasing, the TENG changes into the state (ii) and triboelectric layers separate from each other. Based on the electrostatic induction, negative charges on the surface of the silicone rubber will induce the positive charges to flow from the positively triboelectric materials to the electrode on its backside, resulting in electric potential and eventually the electric current in the external circuit. Afterwards, the positive material layer completely separates from the negative one as shown in the state (iii) and the electrode collects more positive charges. Then, as the magnet starts to approach TENG, the state (iv) occurs where the positive charges flow back to the positively triboelectric layer, leading to the reverse current. Thus, the TENG can generate signal along with the rotation. Similarly, as the magnet slides in the acrylic tube, the distribution of magnetic flux changes in the coil and there generates the induced current to impede this change according to Lenz's law (Fig. 2c).

For TENG's contact-separation mode, obtaining the more transferred charge is the key to improve its output performance. Thus, the main factors affecting voltage output include material type, texture as well as geometric dimension. To enhance the output, the TENG with five different negatively triboelectric materials are tested under 1.0 Hz compression, where the positive material is Ni-cloth and the contact area is constrained to 6 cm^2. The compression test is conducted by the customized compressing machine and the force is regulated by the force sensor as shown in Fig. S1. Compared to other materials such as PTFE and FEP, the result indicates that silicone rubber shows a better output performance (Fig. 2d). Although the increase of contact area will lead to the improved output (Fig. S2), silicone rubber with an area of 7.5 cm^2 is selected due to the limitation of device size. In this paper, sandpapers of different roughness are used to form the micro-pattern on the surface of silicone rubber. As depicted in Fig. 2e, after applying the sandpaper with 500–3000 mesh, the output voltage under the same condition is apparently improved from 20 V to 32 V. The performance improvement is more than 50% compared to the one without any surface treatment and the reason is that the micro-pattern as shown in Fig. S3a enhances the contact area. Besides, the stacked structure with several TENG units connected in parallel is used to improve the output performance as well as for rotational direction (Fig. S3b). The performance of devices with different TENG units in parallel is also verified and the result reflects that the output increases obviously and the voltage of three-stack structure can be doubled to 62 V (Fig. 2f). The short-circuit current and transferred charge of the parallel TENGs are shown in Fig. S4. The working mechanism and the surface charge potential distribution are then theoretically analyzed by finite-element method simulation using the COMSOL Multiphysics software (Fig. 2g–i).

The electrical output performance of the single TENG or EMG unit under different frequencies is measured based on the compression machine to verify the effect of the gear pair. The voltage and current outputs of the EMG unit at four different frequencies are plotted in Fig. 3a. It can be found that the open-circuit voltage increases from 0.14 V to 0.5 V as the rotation frequency increases, while the current increases from 10 mA to 55 mA. The relationship of the power with different load resistances among the EMG unit can be found in Fig. 3b. Under different frequencies, the average output power of the component reaches the peak value at the external resistance of 150 Ω, reaching 0.26 mW, 0.68 mW, 1.02 mW, and 1.88 mW, respectively. The reason for this phenomenon is that the speed of the coil to cut the induction line has a significant effect on power according to Faraday's law. For a single

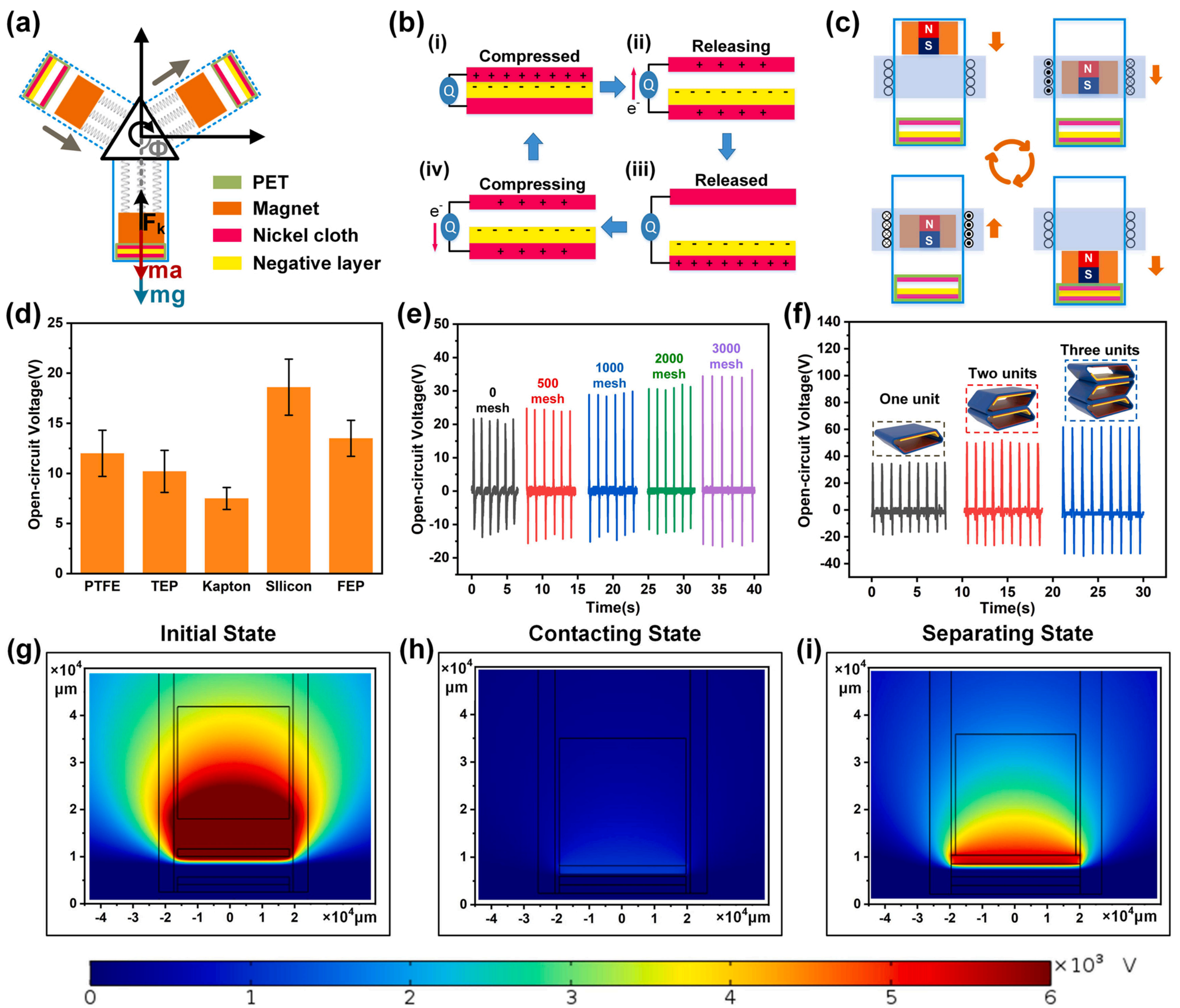

Fig. 2. Optimization of the output performance for TENG-EMG hybrid generator. (a) Schematic diagram to depict the three motion states of the single cylinder: Bottom, fully contact; Left, separating; Right, approaching. (b) Working principle of the TENG structure. (c) Working mechanism of EMG under sliding mode generating varying electrical flux upon the motion of the magnet. (d) Average peak voltages of TENGs when different materials are applied as the negative friction layer. (e) Open-circuit voltages of the TENG with different surface treatments, where 0 mesh presents no treatment and others mean the surface is treated by sandpapers with different meshes. (f) Open-circuit voltages of the TENG units with different layer numbers. (g)–(i) Finite element model simulation of TENG working mechanism using COMSOL Multiphysics software.

TENG, the voltage for 1–4 Hz increases from 35 V to 60 V, while the current increases from 4 μA to 6 μA (Fig. 3d). The average output power of the TENG component under different frequencies reaches the peak value under the external resistance of about 15 MΩ, which is much higher than EMG. Compared to the 1 Hz condition, the TENG compressed with 4 Hz shows about double power approaching to 80.2 μW (Fig. 3e). Then, a capacitor (33 μF, 16 V) has been charged by EMG and TENG respectively (Fig. 3c and f). Similar to the aforementioned result, the capacitor can be charged more quickly under a higher frequency. Also, the result indicates that the maximum value of the capacitor is related to working frequency for EMG and it seems that the TENG with high output voltage can charge the capacitor more quickly.

The characterization of EMG or TENG identifies the gear pear's effect on electrical performance. Thus, the hybrid generator with different gear pairs is used to further verify the performance where the testing system in Fig. S5 with a stepper motor is utilized to mimic different working conditions of the waterwheel and windmill. The waterflow always flows slowly and low frequency causes the issue for energy collection. Hence, gear pairs with different transmission ratios (1:1–1:5) are arranged to accelerate the rotation speed of the hybrid generator where the motor keeps 0.5 Hz rotating. The measured TENG output indicates the hybrid generator can be accelerated by the gear pair and electrical performance is improved largely as well. As for the wind speed detection, there require devices for a larger sensing range (even 40 m/s for typhoon). Here, the hybrid generator realizes 10 Hz detection (Fig. 3g) with the help of gear pair (5:1 transmission ratio). Noticeably, as the device performs 2 Hz and 2.5 Hz rotation, there occur two voltage peaks for one cycle, whereas the 2.5 Hz condition exhibits a smaller value for the second peaks. The reason for this phenomenon is that the combination of inertial force, centrifugal force, and gravity leads the magnet to contact the TENG structure twice in a single cycle. The detailed discussion can be found in Fig. S6 and Supplementary materials Note 2, and the effect to rotation sensing can be avoided by voltage threshold. As depicted in Fig. 3h, the capacitors with 2.2 μF, 10 μF, and 33 μF are charged by three-stack TENG under 1 Hz rotation where the 2.2 μF capacitor shows the quickest charging capacity. The application

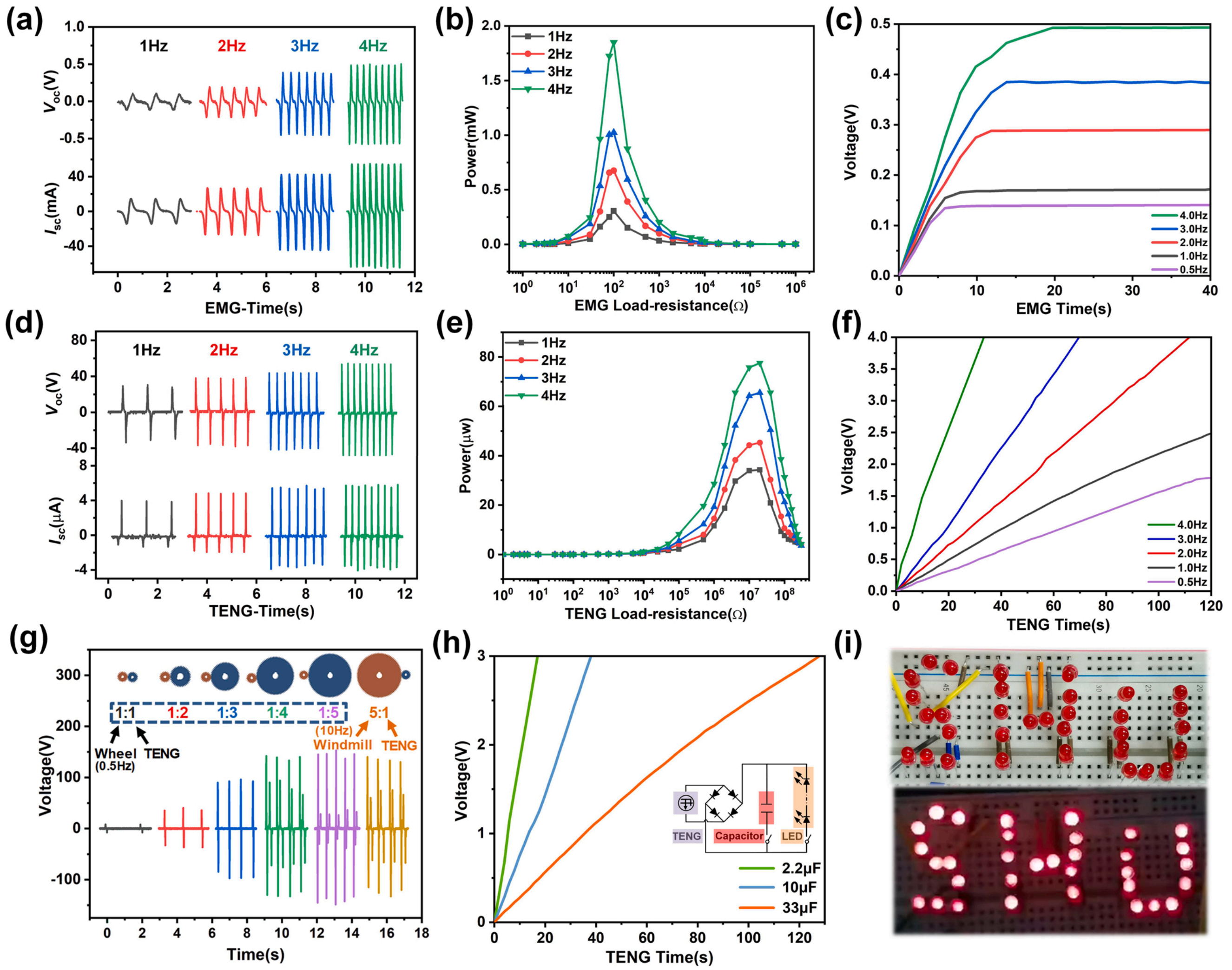

Fig. 3. Electrical output characteristics of the TENG-EMG hybrid generator. (a) Open-circuit voltages and currents for singular EMG activated by different frequencies. (b) Peak powers with different load resistances for the singular EMG. (c) Measured voltages of a 33 μF capacitor charged by EMG. (d) Open-circuit voltages and currents for singular TENG unit activated by different frequencies. (e) Peak powers with different load resistances for TENG. (f) Measured voltages of a 33 μF capacitor charged by TENG. (g) Output characteristics of TENG at different transmission ratios (waterwheel rotational frequency: 0.5 Hz, windmill rotational frequency: 10 Hz). (h) Commercial capacitors with different capacitances are charged by TENG under 1 Hz cyclic compression. The inset is the schematic diagram of the system for capacitor charging. (i) Photo of the LEDs lighted up by TENG.

of the TENG component for energy harvesting is further verified after charging the capacitor. 33 LEDs forming “SHU” are lighted up by the TENG with the circuit in Fig. 3h. Besides, the mechanical durability of the TENG is one of the important factors for both energy harvesting and self-powered sensing applications. Thus, the durability experiment is carried out, where the device is driven by a constant frequency (1.0 Hz). The output voltages in Fig. S7 exhibit negligible changes even though after the usage of 5000 cycles.

As shown in Fig. 4a–b, the real-time wind speed and direction are demonstrated based on the proposed TENG-EMG hybrid generator with a gear pair and windmill. The basic working principle of the sensory system is that microcontroller unit (MCU) with the related circuit detects the real-time signal of the single TENG and then it calculates the time interval to obtain the signal frequency. Noticeably, the signal frequency is equal to the rotation frequency of the hybrid generator. Thus, the real-time wind speed will be given on the screen based on $V_{wind} = 2\pi ifL$, where f is the rotation frequency, i is the transmission ratio, and $L = 200$ mm is the radius of the windmill. The hybrid generator driven by a motor with different rotation speeds is demonstrated to verify the accuracy and as illustrated in Fig. S8a and Movie S1. The device accomplishes an accuracy of more than 97% compared to the rotation speed given by the motor. After integrated with a gear pair (5:1 transmission ratio), the windmill is driven by a blower with different flow rates (from 3 m/s to 10 m/s), and the real-time signal also reflects the time interval between two peaks will decrease along with the increase of the flow speed (Fig. S8b and c). Thus, the sensory system successes to show the real-time speed on the screen (Fig. 4c and Movie S2). Besides, the detected speed also matches with the commercial sensor well (Fig. S8d), showing the good performance in self-powered wind speed monitoring. Here, the as-fabricated device can detect in a speed range up to 15 m/s and it can further be improved by adjusting the spring stiffness or the transmission ratio of the gears. The direction of rotation can also be sensed by connecting three TENG units of different tubes in parallel. As shown in Fig. 4d and Movie S3, the output characteristics of the device driven by two different frequencies (1.0 Hz and 1.5 Hz) in clockwise (CW) and anticlockwise (ACW) states are tested. The result shows that the rotation direction of the device can be recognized by the electrical signal, i.e., incremental peak voltages for CW and decremental peak voltages for ACW.

Supplementary material related to this article can be found online at doi:10.1016/j.nanoen.2021.106501.

As shown in Figs. 4e and S9, two hybrid generators with windmill

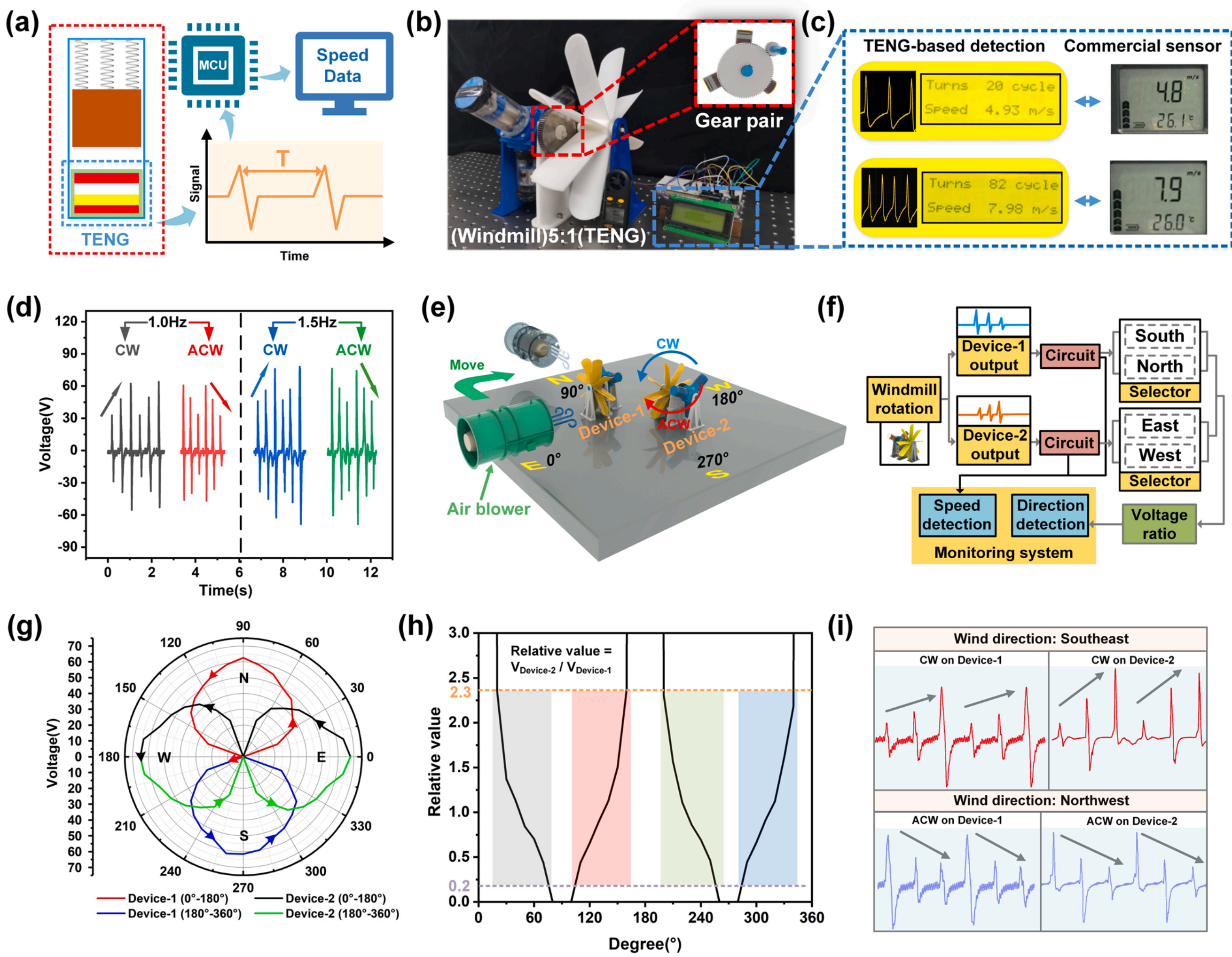

Fig. 4. Demonstration of wind speed and direction detection. (a) Schematic diagram of the self-powered fluid speed measuring system. (b) Device for detecting the wind speed in real time, where the sensing range is expanded by the gear pair with a 5:1 transmission ratio. (c) The result for wind speed detection and the value for commercial sensor. (d) Voltage outputs of TENG for both clockwise (CW) and anticlockwise (ACW). The directions of CW and ACW are defined by facing the windmill. (e) Layout and (f) schematic diagram of the wind speed and orientation monitoring system with two hybrid generators. (g) Peak voltages of TENGs in two hybrid generators driven by the blower with the angle of 0–360°. (h) The TENG voltage outputs of two hybrid generators to distinguish the rotational direction. (i) Relationship of blowing orientation versus relative value. The relative value represents peak voltage ratio of device-1 and device-2, and shadow areas mean the range of 22.5–67.5°, 112.5–157.5°, 202.5–247.5°, and 292.5–337.5°.

marked as device-1 and device-2 are applied to detect both wind speed and direction for weather monitoring. And they are perpendicular to each other and placed on the platform. The basic strategy for determining the wind direction is that the rotation directions can be obtained by comparing the respective signal output of two devices as shown in Fig. 4f. The tests are conducted by starting from the initial position (0°, east) and the blower rotates clockwise slowly at an interval of 10° to obtain the signal outputs of two devices. For a single device, the rotational speed driven by the wind at different orientations shows the specific performance as shown in Fig. S10a. Due to the perpendicular layout, device-2 shows the largest output at first, whereas device-1 has the lowest output voltage. Meanwhile, the output of device-2 decreases with wind direction from 0° to 90° and increases from 90° to 180°. The device-1 shows the reverse trend. In general, the characteristic of a single device with wind from 0° to 360° seems to be a sine wave, and the sine waves for the two devices have a 90° phase difference. The output for different wind directions has been tested 5 times and then plotted in Fig. 4g. By using the voltage ratio of two devices, i.e., $V_{Device-2}/V_{Device-1}$, the relative value can be utilized to improve the sensing accuracy (Fig. 4h). For instance, the lower limit of shadow area ($V_{Device-2}/V_{Device-1} = 0.2$) represents 67.5°, 157.5°, 247.5° and 337.5° while the higher limit ($V_{Device-2}/V_{Device-1} = 2.3$) is for 22.5°, 112.5°, 202.5°and 292.5°. Notably, the relative value in each 180° has the identical trend and the detailed direction can be distinguished based on the rotation direction of the device. As shown in Figs. 4i and S10b, the wind from southeast and northwest causes the device to rotate in different directions. Therefore, the sensory system for wind direction detection can be constructed based on combining two TENG-EMG hybrid generators.

As for the waterflow detection, the flow rate in the river is usually below 0.5 m/s and heavy rainfall for a short period tends to increase the flow rate rapidly. Thus, the as-fabricated hybrid generator is compatible with the waterflow speed monitoring as well. The real-time speed and the total rotation distance of the waterwheel have been demonstrated as shown in Fig. 5a, where the waterwheel is driven by a small pump. The real-time flow speed of a constant (about 1.15 m/s) and variable flow rates (from 0.5 m/s to 1.8 m/s) are validated in Movies S4 and S5. Similarly, as the speed reaches the warning range, the TENG unit realizes the output of the warning signal as shown in Fig. 5b. Herein, it is possible for the hybrid generator in environment monitoring applications such as rainfall measurement and waterflow detection. The TENG-

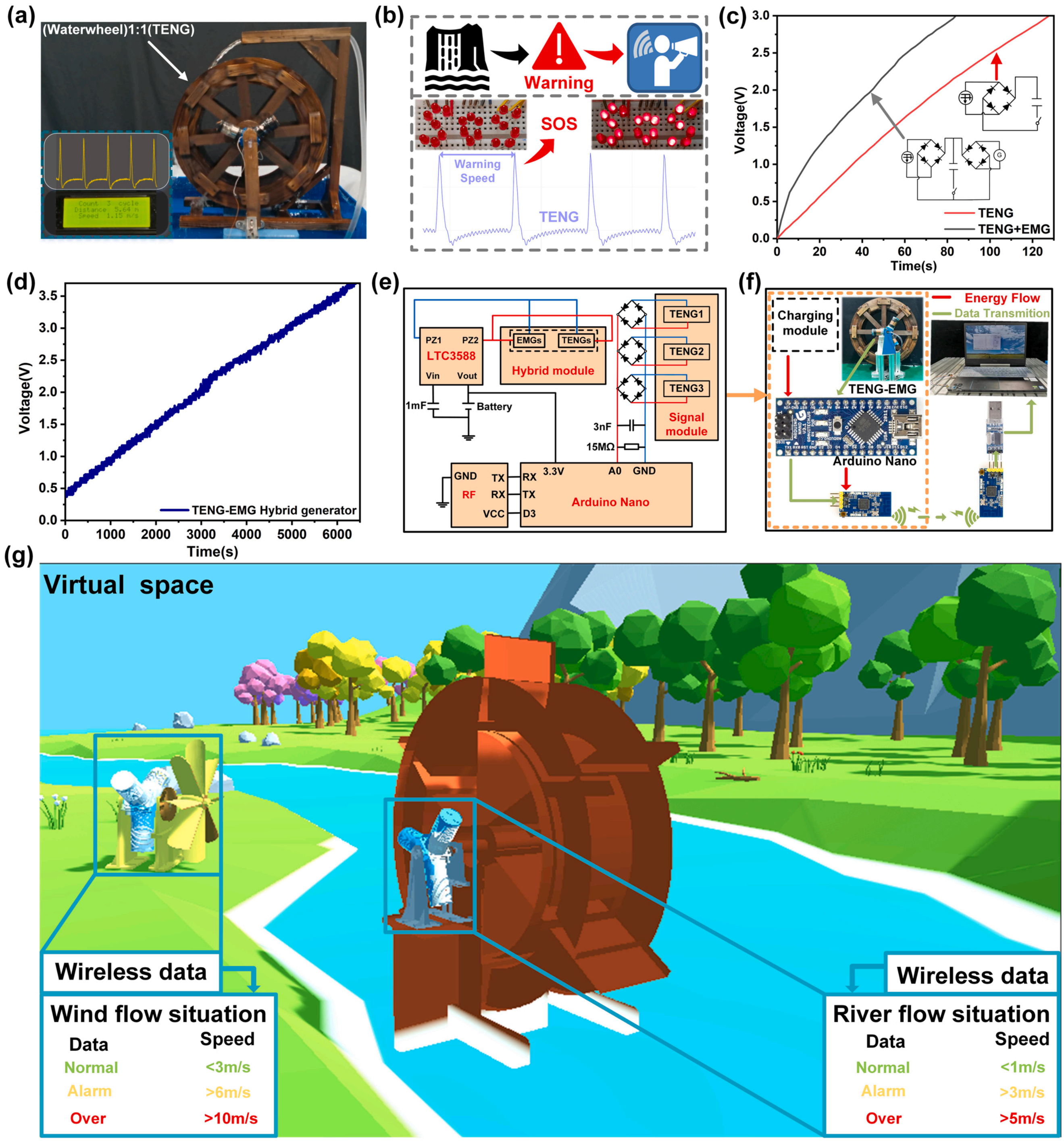

Fig. 5. Demonstration of self-sustainable wireless sensing system. (a) The self-powered sensor based on hybrid generator for detecting the waterflow speed. (b) The schematic diagram for waterflow speed exceeding the limit to generate an alert. (c) Charging commercial capacitor of 33 μF using TENG-EMG hybrid generator. (d) Charging for a lithium-ion battery using the hybrid generator. (e) Diagram of charging circuit for wireless sensing system. (f) Hardware of (e). (g) Illustration diagram for harvesting fluid energy for unmanned environment monitoring.

EMG hybrid generator with the waterwheel and windmill have shown good accuracy as well as sensitivity in the flow speed measurement. Combined with the high current of EMG and the high voltage of TENG, the hybrid generator could be connected in parallel to charge the 33 μF capacitor. Here, a single TENG-EMG module (three-stack TENG and one EMG) can charge the capacitor to the 3 V in 98 s while a single TENG structure needs 135 s (Fig. 5c) under 1 Hz rotation. The experimental results show that the hybrid module has a stronger energy collection capability than single EMG or TENG, which shows the superior performance of the hybrid energy collector, and the device has the potential to meet the demand of power supply for the IoT-based monitoring system. The hybrid generator is then applied to charge the commercial lithium-ion battery (3.7 V, 45 mA h) at a frequency of 1 Hz. It takes less than 7000 s to charge the battery from 0.7 V to 3.7 V (Fig. 5d).

Supplementary material related to this article can be found online at doi:10.1016/j.nanoen.2021.106501.

Herein, the self-powered sensing can be realized based on the charged battery with the power management module to support the operation of MCU and wireless transmission module. To decrease the power density, power management circuits are designed for the wireless sensory system as shown in Fig. 5e. The hybrid generator provides AC voltage to PZ1 and PZ2 of the power management chip (LTC 3588) and the AC voltage will be rectified to charge a capacitor of 1 mF. Here, the low dropout regulator (LDO) and power LED in Arduino Nano are removed for decreasing the energy consumption and the input voltage can be decreased from 5 V to 3.3 V [8]. Furthermore, as the RF transceiver accounts for the large energy consumption, it is set to be intermittently powered to reduce the energy consumption, which can be achieved through Arduino Nano codes or the manual switch. Thus, under-voltage lockout (UVLO) in the chip will work from 3.67 V to 5.05 V as the V_{out} is defined as 3.3 V. LTC 3588 outputs the voltage through V_{out}, where a battery is utilized to store the output energy for powering the Arduino Nano. The TENG of the hybrid generator outputs stable voltage signals to the A0 through the filtering and rectifier circuit, and then, the signal can be read by MCU. Here, the filter capacity is 3 nF and the adjustable resistance is 15 MΩ to adjust the voltage value. The digital signals received by Arduino Nano are delivered through the RF transceiver port (Bluetooth, DL-20 CC2530). As depicted in Fig. 5f, the host terminal has another RF transceiver where a laptop computer is to receive and display wireless data. Movie S6 and Fig. S11 demonstrate the wireless sensory system for waterflow speed measurement, where both the charging and sensing can be intermittently achieved. The virtual scenarios of waterflow and wind monitoring are shown in Fig. 5g. The gear-based structure can effectively convert and collect the mechanical energy of water at a low flow rate while it can enlarge the sensing range of the wind speed detection. The normal velocity of wind and waterflow can satisfy the energy requirements for wireless transmission, while the real-time wind and waterflow speed can be monitored. Thus, the proposed TENG-EMG hybrid generator shows a huge potential in the environmental monitoring for the unmanned weather station, disaster warning as well as meteorological record.

Supplementary material related to this article can be found online at doi:10.1016/j.nanoen.2021.106501.

3. Conclusions

In summary, we have demonstrated a tri-cylinder-like TENG-EMG hybrid generator for fluid energy harvesting and self-powered wireless sensing system application in this paper. The spring-magnet structure is arranged in each cylinder to achieve the successive sliding to activate the sandwiched TENG and generate the induced current for EMG as the device's rotation. Gear pairs with different transmission ratios are further utilized for the hybrid generator to boost the output and expand the sensing range based on enlarging the rotational frequency for low frequency and slowing down for higher frequency, respectively. The experimental result shows more than twice and six times outputs are realized by gear pair for TENG and EMG respectively under 1 Hz external stimulation, and the recognizable rotational frequency reaches 10 Hz with a transmission ratio of 5:1. The rotation speed and direction detection are realized depending on the signal frequency and voltage sequence since the triboelectric layer number in each cylinder is different. The hybrid generator together with windmill or waterwheel has verified the fluid flow speed detection for weather monitoring and two hybrid generators with vertical layout are developed to distinguish the wind orientation by computing the signal ratio. The hybrid generator is also demonstrated to achieve wireless sensing as EMG boosted by gear pair is sufficient to supply the energy for wireless transmission and TENG works stably for rotation sensing. This self-sustained sensory system shows its potential for unmanned environment monitoring, disaster warning as well as the meteorological record in IoT applications.

4. Methods

4.1. Fabrication of the TENG

PET film is cut into a 30 mm × 30 mm × 1 mm patch and two ends of the patch are bonded together by double-sided tape to form the substrate. Part A and part B of the negatively triboelectric materials (Ecoflex 00-50, Smooth-on) are equally mixed and stirred for 2 min. The mixed silicone rubber is put into the vacuum environment to debubble for 3 min and then poured into the mold with sandpaper at the bottom. A piece of Ni-cloth is placed above the silicone rubber before curing in the oven at 70 °C for 60 min. After demolding, the 30 mm × 25 mm silicone rubber is glued to the PET substrate by Sil-poxy (Smooth-on) and another triboelectric layer cut from the Ni-cloth tape with the same dimension is fixed on the opposite face of PET substrate. The TENG units are bonded together by double-sided tape to construct the two-stack and three-stack TENG structure.

4.2. Fabrication of the TENG-EMG hybrid generator

The central component is designed by 3D software (Solidworks 2016) and then fabricated by the 3D printer (M200 plus, Zortrax). The stretching spring bonded with NbFeB magnet and acrylic pipe with 50 × 100 × 2 mm^3 are fixed to the central component through holt-melt glue. The TENG unit is glued onto a 3D-printed cap and then the cap seals the acrylic pipe to prevent the external factors affecting the output performance. Cu wire with 0.35 mm diameter is wrapped from the middle of each pipe to the distal end for 100 turns to form the electromagnetic coil. The conductive slip ring (MT0522, Moflon) is set at the center axis of the device to avoid the conductive thread winding.

4.3. The electrical measurement

The electrical signals including open-circuit voltage, short-circuit current and transferred charge are observed through an electrometer (Model 6514, Keithley) and recorded by an oscilloscope (DSOX 3034T, Keithley). The customized machine with a crank-link mechanism is applied to compress the TENG structure and the compressing force can be sensed by the force sensor (DF9-40-MY2801). The performance of the hybrid generator with waterwheel or windmill is tested by a probe with 100 MΩ impedance and displayed by the oscilloscope. The flow velocity detections are controlled by the MCU (Arduino Mega 2560) with the concerned processing circuit and the real-time velocity is displayed through LCD. The power management module (LTC3588, LINEAR) together with Arduino Nano is used to manage the energy charging process for wireless transmission and the commercial anemometer (AT816, Smart Sensor) is applied to get the standard wind speed.

CRediT authorship contribution statement

Zhang Quan: Data curation, Writing – original draft. **Long Li, Tianhong Wang:** Validation, Software, Investigation. **Yichen Jiang:** Data curation, Visualization. **Yingzhong Tian:** Resources. **Tao Jin:** Conceptualization, Methodology. **Tao Yue:** Funding acquisition, Supervision. **Chengkuo Lee:** Writing – review & editing.

Declaration of Competing Interest

The authors declare that they have no known competing financial interests or personal relationships that could have appeared to influence the work reported in this paper.

Data availability

The data that support the findings of this study are available from the corresponding authors upon reasonable request.

Acknowledgements

This work is supported by the National Natural Science Foundation of China (Grant no. 61973207), Shanghai Rising-Star Program under Grant of 20QA1403900, the Natural Science Foundation of Shanghai (Grant nos. 21ZR1423000 and 19ZR1474000), and the State Key Laboratory of Mechanics and Control of Mechanical Structures (Nanjing University of Aeronautics and Astronautics, Grant no. MCMS-E-0320G01).

Appendix A. Supplementary material

Supplementary data associated with this article can be found in the online version at doi:10.1016/j.nanoen.2021.106501.

References

[1] J. Wang, H.L. Zhang, Y.H. Xie, Z.C. Yan, Y. Yuan, L. Huang, X.J. Cui, M. Gao, Y. J. Su, W.Q. Yang, Y. Lin, Smart network node based on hybrid nanogenerator for self-powered multifunctional sensing, Nano Energy 33 (2017) 418–426.
[2] Q.F. Shi, H. Wang, H. Wu, C.K. Lee, Self-powered triboelectric nanogenerator buoy ball for applications ranging from environment monitoring to water wave energy farm, Nano Energy 40 (2017) 203–213.
[3] H. Lin, M. He, Q. Jing, W. Yang, S. Wang, Y. Liu, Y. Zhang, J. Li, N. Li, Y. Ma, L. Wang, Y. Xie, Angle-shaped triboelectric nanogenerator for harvesting environmental wind energy, Nano Energy 56 (2019) 269–276.
[4] T. Jin, Z.D. Sun, L. Li, Q. Zhang, M.L. Zhu, Z.X. Zhang, G.J. Yuan, T. Chen, Y. Z. Tian, X.Y. Hou, C. Lee, Triboelectric nanogenerator sensors for soft robotics aiming at digital twin applications, Nat. Commun. 11 (2020) 5381.
[5] S.-J. Park, S. Lee, M.-L. Seol, S.-B. Jeon, H. Bae, D. Kim, G.-H. Cho, Y.-K. Choi, Self-sustainable wind speed sensor system with omni-directional wind based triboelectric generator, Nano Energy 55 (2019) 115–122.
[6] F. Wen, H. Wang, T.Y.Y. He, Q.F. Shi, Z.D. Sun, M.L. Zhu, Z.X. Zhang, Z.G. Cao, Y. B. Dai, T. Zhang, C.K. Lee, Battery-free short-range self-powered wireless sensor network (SS-WSN) using TENG based direct sensory transmission (TDST) mechanism, Nano Energy 67 (2020), 104266.
[7] J.X. Zhu, X.M. Liu, Q.F. Shi, T.Y.Y. He, Z.D. Sun, X.G. Guo, W.X. Liu, O. Bin Sulaiman, B.W. Dong, C. Lee, Development trends and perspectives of future sensors and MEMS/NEMS, Micromachines 11 (2020) 30.
[8] L. Wang, T.Y.Y. He, Z.X. Zhang, L.B. Zhao, C.K. Lee, G.X. Luo, Q. Mao, P. Yang, Q. J. Lin, X. Li, R. Maeda, Z.D. Jiang, Self-sustained autonomous wireless sensing based on a hybridized TENG and PEG vibration mechanism, Nano Energy 80 (2021), 105555.
[9] Q. Shi, Z. Sun, Z. Zhang, C. Lee, Triboelectric nanogenerators and hybridized systems for enabling next-generation IoT applications, Research 2021 (2021), 6849171.
[10] L. Liu, Q.F. Shi, C. Lee, A novel hybridized blue energy harvester aiming at all-weather IoT applications, Nano Energy 76 (2020) 11.
[11] J.J. Luo, F.R. Fan, T. Zhou, W. Tang, F. Xue, Z.L. Wang, Ultrasensitive self-powered pressure sensing system, Extrem. Mech. Lett. 2 (2015) 28–36.
[12] R. Lei, H. Zhai, J. Nie, W. Zhong, Y. Bai, X. Liang, L. Xu, T. Jiang, X. Chen, Z. L. Wang, Butterfly-inspired triboelectric nanogenerators with spring-assisted linkage structure for water wave energy harvesting, Adv. Mater. Technol. 4 (2019), 1800514.
[13] H. Liu, H. Fu, L. Sun, C. Lee, E.M. Yeatman, Hybrid energy harvesting technology: from materials, structural design, system integration to applications, Renew. Sustain. Energy Rev. 137 (2021), 110473.
[14] Z. Wen, H.Y. Guo, Y.L. Zi, M.H. Yeh, X. Wang, J.A. Deng, J. Wang, S.M. Li, C.G. Hu, L.P. Zhu, Z.L. Wang, Harvesting broad frequency band blue energy by a triboelectric-electromagnetic hybrid nanogenerator, ACS Nano 10 (2016) 6526–6534.
[15] L. Zhang, B. Meng, Y. Xia, Z. Deng, H. Dai, P. Hagedorn, Z. Peng, L. Wang, Galloping triboelectric nanogenerator for energy harvesting under low wind speed, Nano Energy 70 (2020), 104477.
[16] T. Jiang, Y.Y. Yao, L. Xu, L.M. Zhang, T.X. Xiao, Z.L. Wang, Spring-assisted triboelectric nanogenerator for efficiently harvesting water wave energy, Nano Energy 31 (2017) 560–567.
[17] Q.F. Shi, H. Wu, H. Wang, H.X. Wu, C.K. Lee, Self-powered gyroscope ball using a triboelectric mechanism, Adv. Energy Mater. 7 (2017), 1701300.
[18] F.R. Fan, Z.Q. Tian, Z.L. Wang, Flexible triboelectric generator!, Nano Energy 1 (2012) 328–334.
[19] Z.L. Wang, On Maxwell's, displacement current for energy and sensors: the origin of nanogenerators, Mater. Today 20 (2017) 74–82.
[20] Z.L. Wang, Triboelectric nanogenerators as new energy technology and self-powered sensors – principles, problems and perspectives, Faraday Discuss. 176 (2014) 447–458.
[21] G. Zhu, J. Chen, T.J. Zhang, Q.S. Jing, Z.L. Wang, Radial-arrayed rotary electrification for high performance triboelectric generator, Nat. Commun. 5 (2014) 3426.
[22] N. Zhai, Z. Wen, X. Chen, A. Wei, M. Sha, J. Fu, Y. Liu, J. Zhong, X. Sun, Blue energy collection toward all-hours self-powered chemical energy conversion, Adv. Energy Mater. 10 (2020), 2001041.
[23] K. Barri, P. Jiao, Q. Zhang, J. Chen, Z.L. Wang, A.H. Alavi, Multifunctional meta-tribomaterial nanogenerators for energy harvesting and active sensing, Nano Energy 86 (2021), 106074.
[24] S. Yong, J. Wang, L. Yang, H. Wang, H. Luo, R. Liao, Z.L. Wang, Auto-switching self-powered system for efficient broad-band wind energy harvesting based on dual-rotation shaft triboelectric nanogenerator, Adv. Energy Mater. 11 (2021), 2101194.
[25] Z. Lin, J. Chen, X. Li, Z. Zhou, K. Meng, W. Wei, J. Yang, Z.L. Wang, Triboelectric nanogenerator enabled body sensor network for self-powered human heart-rate monitoring, ACS Nano 11 (2017) 8830–8837.
[26] S.T. Liu, H. Wang, T.Y.Y. He, S.R. Dong, C.K. Lee, Switchable textile-triboelectric nanogenerators (S-TENGs) for continuous profile sensing application without environmental interferences, Nano Energy 69 (2020), 104462.
[27] Y.C. Lai, Y.C. Hsiao, H.M. Wu, Z.L. Wang, Waterproof fabric-based multifunctional triboelectric nanogenerator for universally harvesting energy from raindrops, wind, and human motions and as self-powered sensors, Adv. Sci. 6 (2019), 1801883.
[28] X. Pu, L.X. Li, H.Q. Song, C.H. Du, Z.F. Zhao, C.Y. Jiang, G.Z. Cao, W.G. Hu, Z. L. Wang, A self-charging power unit by integration of a textile triboelectric nanogenerator and a flexible lithium-ion battery for wearable electronics, Adv. Mater. 27 (2015) 2472–2478.
[29] B.W. Dong, Y.Q. Yang, Q.F. Shi, S.Y. Xu, Z.D. Sun, S.Y. Zhu, Z.X. Zhang, D. L. Kwong, G.Y. Zhou, K.W. Ang, C.K. Lee, Wearable triboelectric-human-machine interface (THMI) using robust nanophotonic readout, ACS Nano 14 (2020) 8915–8930.
[30] B.W. Dong, Q.F. Shi, T.Y.Y. He, S.Y. Zhu, Z.X. Zhang, Z.D. Sun, Y.M. Ma, D. L. Kwong, C. Lee, Wearable triboelectric/aluminum nitride nano-energy-nano-system with self-sustainable photonic modulation and continuous force sensing, Adv. Sci. 7 (2020), 1903636.
[31] T.Y.Y. He, H. Wang, J.H. Wang, X. Tian, F. Wen, Q.F. Shi, J.S. Ho, C.K. Lee, Self-sustainable wearable textile nano-energy nano-system (NENS) for next-generation healthcare applications, Adv. Sci. 6 (2019), 1901437.
[32] P. Jiao, Emerging artificial intelligence in piezoelectric and triboelectric nanogenerators, Nano Energy 88 (2021), 106227.
[33] Q.F. Shi, Z.X. Zhang, T. Chen, C.K. Lee, Minimalist and multi-functional human machine interface (HMI) using a flexible wearable triboelectric patch, Nano Energy 62 (2019) 355–366.
[34] G. Tang, Q.F. Shi, Z.X. Zhang, T.Y.Y. He, Z.D. Sun, C. Lee, Hybridized wearable patch as a multi-parameter and multi-functional human-machine interface, Nano Energy 81 (2021), 105582.
[35] F. Wen, Z.D. Sun, T.Y.Y. He, Q.F. Shi, M.L. Zhu, Z.X. Zhang, L.H. Li, T. Zhang, C. K. Lee, Machine learning glove using self-powered conductive superhydrophobic triboelectric textile for gesture recognition in VR/AR applications, Adv. Sci. 7 (2020), 2000261.
[36] C.K. Qiu, F. Wu, Q.F. Shi, C.K. Lee, M.R. Yuce, Sensors and control interface methods based on triboelectric nanogenerator in IoT applications, IEEE Access 7 (2019) 92745–92757.
[37] C. Zhang, Z. Zhao, O. Yang, W. Yuan, L. Zhou, X. Yin, L. Liu, Y. Li, Z.L. Wang, J. Wang, Bionic-fin-structured triboelectric nanogenerators for undersea energy harvesting, Adv. Mater. Technol. (2020), 2000531.
[38] T. Chen, Q.F. Shi, M.L. Zhu, T.Y.Y. He, L.N. Sun, L. Yang, C. Lee, Triboelectric self-powered wearable flexible patch as 3D motion control interface for robotic manipulator, ACS Nano 12 (2018) 11561–11571.
[39] T. Chen, Q.F. Shi, M.L. Zhu, T.Y.Y. He, Z. Yang, H.C. Liu, L.N. Sun, L. Yangt, C. Lee, Intuitive-augmented human-machine multidimensional nano-manipulation terminal using triboelectric stretchable strip sensors based on minimalist design, Nano Energy 60 (2019) 440–448.
[40] X. Chen, Z. Ren, M. Han, J. Wan, H. Zhang, Hybrid energy cells based on triboelectric nanogenerator: from principle to system, Nano Energy 75 (2020), 104980.
[41] H.Y. Shao, P. Cheng, R.X. Chen, L.J. Xie, N. Sun, Q.Q. Shen, X.P. Chen, Q.Q. Zhu, Y. Zhang, Y.N. Liu, Z. Wen, X.H. Sun, Triboelectric electromagnetic hybrid generator for harvesting blue energy, Nano-Micro Lett. 10 (2018) 54.
[42] Y. Feng, X. Liang, J. An, T. Jiang, Z.L. Wang, Soft-contact cylindrical triboelectric-electromagnetic hybrid nanogenerator based on swing structure for ultra-low frequency water wave energy harvesting, Nano Energy 81 (2021), 105625.
[43] T.C. Zhao, S.L. Cao, S. Yang, R. Guo, S.B. Sang, H.L. Zhang, A self-powered counter/timer based on a clock pointer-like frequency-tunable triboelectric nanogenerator for wind speed detecting, Nano Energy 65 (2019), 104025.
[44] P.H. Wang, L. Pan, J.Y. Wang, M.Y. Xu, G.Z. Dai, H.Y. Zou, K. Dong, Z.L. Wang, An ultra-low-friction triboelectric-electromagnetic hybrid nanogenerator for rotation energy harvesting and self-powered wind speed sensor, ACS Nano 12 (2018) 9433–9440.
[45] W.Q. Yang, J. Chen, G. Zhu, J. Yang, P. Bai, Y.J. Su, Q.S. Jing, X. Cao, Z.L. Wang, Harvesting energy from the natural vibration of human walking, ACS Nano 7 (2013) 11317–11324.
[46] G. He, Y. Luo, Y. Zhai, Y. Wu, J. You, R. Lu, S. Zeng, Z.L. Wang, Regulating random mechanical motion using the principle of auto-winding mechanical watch for driving TENG with constant AC output – an approach for efficient usage of high entropy energy, Nano Energy 87 (2021), 106195.
[47] T.X. Xiao, X. Liang, T. Jiang, L. Xu, J.J. Shao, J.H. Nie, Y. Bai, W. Zhong, Z.L. Wang, Spherical triboelectric nanogenerators based on spring-assisted multilayered

structure for efficient water wave energy harvesting, Adv. Funct. Mater. 28 (2018), 1802634.
[48] L. Jin, W.L. Deng, Y.C. Su, Z. Xu, H. Meng, B. Wang, H.P. Zhang, B.B. Zhang, L. Zhang, X.B. Xiao, M.H. Zhu, W.Q. Yang, Self-powered wireless smart sensor based on maglev porous nanogenerator for train monitoring system, Nano Energy 38 (2017) 185–192.
[49] M.Y. Shi, H.X. Wu, J.X. Zhang, M.D. Han, B. Meng, H.X. Zhang, Self-powered wireless smart patch for healthcare monitoring, Nano Energy 32 (2017) 479–487.
[50] Y.D. Chen, Y. Cheng, Y. Jie, X. Cao, N. Wang, Z.L. Wan, Energy harvesting and wireless power transmission by a hybridized electromagnetic-triboelectric nanogenerator, Energy Environ. Sci. 12 (2019) 2678–2684.
[51] L.M. Zhao, Q. Zheng, H. Ouyang, H. Li, L. Yan, B.J. Shi, Z. Li, A size-unlimited surface microstructure modification method for achieving high performance triboelectric nanogenerator, Nano Energy 28 (2016) 172–178.
[52] H. Zhang, T. Wan, B.W. Cheng, W. Li, S.Y. Wang, X.J. Li, Polyvinylidene fluoride injection electrets: preparation, characterization, and application in triboelectric nanogenerators, J. Mater. Res. Technol.-JMRT 9 (2020) 12643–12653.
[53] Z. Wang, L. Cheng, Y.B. Zheng, Y. Qin, Z.L. Wang, Enhancing the performance of triboelectric nanogenerator through prior-charge injection and its application on self-powered anticorrosion, Nano Energy 10 (2014) 37–43.
[54] I. Kim, H. Roh, W. Choi, D. Kim, Air-gap embedded triboelectric nanogenerator via surface modification of non-contact layer using sandpapers, Nanoscale 13 (2021) 8837–8847.
[55] Q. Zhang, E.S. Kim, Micromachined energy-harvester stack with enhanced electromagnetic induction through vertical integration of magnets, J. Microelectromech. Syst. 24 (2015) 384–394.
[56] H. Park, Vibratory electromagnetic induction energy harvester on wheel surface of mobile sources, Int. J. Precis. Eng. Manuf.-Green Technol. 4 (2017) 59–66.
[57] T.S. Almoneef, O.M. Ramahi, Metamaterial electromagnetic energy harvester with near unity efficiency, Appl. Phys. Lett. 106 (2015), 153902.
[58] L.L. Zhou, D. Liu, S.X. Li, Z.H. Zhao, C.L. Zhang, X. Yin, L. Liu, S.N. Cui, Z.L. Wang, J. Wang, Rationally designed dual-mode triboelectric nanogenerator for harvesting mechanical energy by both electrostatic induction and dielectric breakdown effects, Adv. Energy Mater. 10 (2020) 8.
[59] M. Zenkiewicz, T. Zuk, E. Markiewicz, Triboelectric series and electrostatic separation of some biopolymers, Polym. Test. 42 (2015) 192–198.
[60] D. Liu, L.L. Zhou, S.X. Li, Z.H. Zhao, X. Yin, Z.Y. Yi, C.L. Zhang, X.Y. Li, J. Wang, Z. L. Wang, Hugely enhanced output power of direct-current triboelectric nanogenerators by using electrostatic breakdown effect, Adv. Mater. Technol. 5 (2020), 2000289.
[61] M. Rezaeisaray, M. El Gowini, D. Sameoto, D. Raboud, W. Moussa, Low frequency piezoelectric energy harvesting at multi vibration mode shapes, Sens. Actuators A-Phys. 228 (2015) 104–111.
[62] S. Mehraeen, S. Jagannathan, K.A. Corzine, Energy harvesting from vibration with alternate scavenging circuitry and tapered cantilever beam, IEEE Trans. Ind. Electron. 57 (2010) 820–830.
[63] B. Montazer, U. Sarma, Design and optimization of quadrilateral shaped PVDF cantilever for efficient conversion of energy from ambient vibration, IEEE Sens. J. 18 (2018) 3977–3988.
[64] L. Feng, G. Liu, H. Guo, Q. Tang, X. Pu, J. Chen, X. Wang, Y. Xi, C. Hu, Hybridized nanogenerator based on honeycomb-like three electrodes for efficient ocean wave energy harvesting, Nano Energy 47 (2018) 217–223.
[65] A. Chandrasekhar, V. Vivekananthan, S.J. Kim, A fully packed spheroidal hybrid generator for water wave energy harvesting and self-powered position tracking, Nano Energy 69 (2020), 104439.
[66] C. Hou, T. Chen, Y.F. Li, M.J. Huang, Q.F. Shi, H.C. Liu, L.N. Sun, C. Lee, A rotational pendulum based electromagnetic/triboelectric hybrid-generator for ultra-low-frequency vibrations aiming at human motion and blue energy applications, Nano Energy 63 (2019), 103871.
[67] Y. Fang, T. Tang, Y. Li, C. Hou, F. Wen, Z. Yang, T. Chen, L. Sun, H. Liu, C. Lee, A high-performance triboelectric-electromagnetic hybrid wind energy harvester based on rotational tapered rollers aiming at outdoor IoT applications, iScience 24 (2021), 102300.

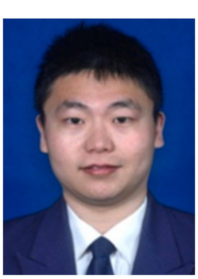

Quan Zhang received the B.S. degree in Mechanical Manufacturing and Automation and the Ph.D. degree in Mechatronics from Nanjing University of Aeronautics and Astronautics in 2009 and 2014, respectively. He is currently an Associate Professor with the School of Mechatronic Engineering and Automation, Shanghai University. He has won the rising-star program of Shanghai. His research interests include triboelectric nanogenerator, robotic sensing and actuating with smart materials.

Long Li received the Ph.D. degree in Mechanical Design and Theory in 2013 from Harbin Institute of Technology. He has joined Shanghai University since 2013, and now he is with School of Artificial Intelligence, School of Mechatronic Engineering and Automation, and Shanghai Key Laboratory of Intelligent Manufacturing and Robotics at the same university. His research interests include triboelectric nanogenerator, intelligent structure and sensor, soft robot, and biomimetic robot.

Tianhong Wang received the B.S. degree in mechanical design manufacturing and automation from Zhejiang Sci-Tech University in 2018. He is currently pursuing the Ph.D. degree in School of Mechatronic Engineering and Automation, Shanghai University. His research interests include triboelectric nanogenerator, soft robot and robotic sensing.

Yichen Jiang received the B.S. degree in mechanical design manufacturing and automation from Zhejiang Sci-Tech University in 2019. He is currently pursuing the master degree in School of Mechatronic Engineering and Automation, Shanghai University. His research interests include triboelectric nanogenerator, energy harvester and robotic sensing.

Yingzhong Tian received the Ph.D. degree in Mechanical manufacture and automation from Shanghai University in 2007. He is currently a professor with the Shanghai Key Laboratory of Intelligent Manufacturing and Robotics, School of Mechatronic Engineering and Automation, Shanghai University. His research interests include mobile robot, multi-robot systems and image processing.

Tao Jin received the B.S. degree in mechanical design manufacturing and automation from Zhejiang Sci-Tech University in 2017. He is currently pursuing the Ph.D. degree in School of Mechatronic Engineering and Automation, Shanghai University. His research interests include triboelectric nanogenerator, soft robot and robotic sensing.

Tao Yue received the Ph.D. degree in Micro Nano Systems Engineering from Nagoya University, Japan in 2014. He is currently an associate professor in School of Mechatronic Engineering and Automation at Shanghai University, China. His research interests include micro/nano robotics and manipulation, microfluidic devices, precision instruments and bio-mems technologies.

Chengkuo Lee received his Ph.D. degree in Precision Engineering from The University of Tokyo in 1996. Currently, he is the director of Center for Intelligent Sensors and MEMS at National University of Singapore, Singapore. In 2001, he cofounded Asia Pacific Microsystems, Inc., where he was the Vice President. From 2006 to 2009, he was a Senior Member of the Technical Staff at the Institute of Microelectronics, A-STAR, Singapore. He has contributed to more than 380 peer-reviewed international journal articles.